Available online at www.sciencedirect.com
ScienceDirect
International Journal of Heat and Fluid Flow 29 (2008) 1221–1232
International Journal of HEAT AND FLUID FLOW
www.elsevier.com/locate/ijhff

Thermal performance of nanofluid flow in microchannels

Jie Li, Clement Kleinstreuer *

Department of Mechanical and Aerospace Engineering, University of North Carolina, Campus Box 7910, Broungton Hall 4160, Raleigh, NC 27695-7910, USA

Received 5 September 2007; received in revised form 29 December 2007; accepted 8 January 2008
Available online 10 March 2008

Abstract

Two effective thermal conductivity models for nanofluids were compared in detail, where the new KKL (Koo–Kleinstreuer–Li) model, based on Brownian motion induced micro-mixing, achieved good agreements with the currently available experimental data sets. Employing the commercial Navier–Stokes solver CFX-10 (Ansys Inc., Canonsburg, PA) and user-supplied pre- and post-processing software, the thermal performance of nanofluid flow in a trapezoidal microchannel was analyzed using pure water as well as a nanofluid, i.e., CuO–water, with volume fractions of 1% and 4% CuO-particles with $d_p = 28.6$ nm. The results show that nanofluids do measurably enhance the thermal performance of microchannel mixture flow with a small increase in pumping power. Specifically, the thermal performance increases with volume fraction; but, the extra pressure drop, or pumping power, will somewhat decrease the beneficial effects. Microchannel heat sinks with nanofluids are expected to be good candidates for the next generation of cooling devices.
© 2008 Elsevier Inc. All rights reserved.

Keywords: Brownian motion; Micro-mixing; Effective thermal conductivity; Nanofluid flow; Microchannel heat sinks

1. Introduction

Microscale cooling devices, such as microchannel heat sinks, are increasingly important in current and future heat removal applications. Specifically, a coolant flowing through a large number of parallel, micromachined or etched conduits with the purpose to remove heat from and generate uniform temperature distributions in micro-electro-mechanical systems, integrated circuit boards, laser-diode arrays, high-energy mirrors and other compact products with high transient thermal loads. Key is the very large heat transfer surface-to-volume ratio of the devices, leading to high compactness and effectiveness of heat removal. Complementary to that is the use of high thermal performance coolants. Most exciting are new coolants consisting of a combination of a low-volume fraction of nanoparticles (e.g., metals, metal-oxides, or carbon-based material) with a suitable carrier fluid, such as distilled water, engine oil, ethylene glycol. As first demonstrated in 1995 at Argonne National Laboratory, those dilute liquid-particle mixtures, called nanofluids, have exhibited thermal conductivity values 20–150% higher then the ones of the base fluids (Choi, 1995; Chopkar et al., 2007). Over the last seven years numerous experimental and a few theoretical papers appeared, providing nanofluid property measurements and models describing the underlying physics of enhanced thermal conductivities for different nanoparticle-and-liquid pairings.

The effective thermal conductivity (k_{eff}) of any nanofluid depends mainly on the nanoparticle volume fraction, conductivity and diameter, as well as the carrier-fluid temperature and conductivity. Fig. 1 provides a glimpse of the most recent measurements for k_{eff} vs. φ (the volume fraction), considering different temperatures, types of mixtures, and nanoparticle diameters. Metal-oxides (e.g., Al_2O_3, CuO, TiO_2, etc.) were first used in static nanofluid studies (see Masuda et al., 1993; Lee et al., 1999; Zhou and Wang, 2002; Xie et al., 2002; and Chang et al., 2005; among others). However, nanofluids with metals (e.g., Cu, Fe, Au, etc.) or carbon-based materials generated higher k_{eff} values.

* Corresponding author. Tel.: +1 9195155261; fax: +1 9195157968.
E-mail address: ck@eos.ncsu.edu (C. Kleinstreuer).

0142-727X/$ - see front matter © 2008 Elsevier Inc. All rights reserved.
doi:10.1016/j.ijheatfluidflow.2008.01.005

Nomenclature

A_{af}	aspect factor ($=H/W_b$)
A_{ar}	aspect ratio ($=W_b/W_t$)
A_c	area of the channel cross section
A_{bottom}	area of the heated substrate wall
C	constant
C_f	friction coefficient
c_p	specific heat capacity
d	diameter
D_h	hydraulic diameter
H	channel height
k	thermal conductivity
L	channel length
m	constant
Nu	Nusselt number
p	pressure
P	pumping power
Pr	Prandtl number
q''	uniform heat flux
Q	volumetric flow rate
R_b	interfacial thermal resistance
Re	Reynolds number
T	temperature
u, v	velocity
V_N	root-mean-square velocity
W_b	channel bottom width
W_t	channel top width

Greek Letters

α	nanoparticle Biot number
φ	volume fraction
κ_b	Boltzmann constant
μ	dynamic viscosity
ν	kinematic viscosity
θ	thermal resistance
ρ	density

Subscripts

ave	average
eff	effective
f	base fluid
in	inlet
int	interface
m	mean
out	outlet
p	particle
w	wall

For example, Eastman et al. (2001) observed that a nanofluid consisting of 10 nm copper nanoparticles dispersed in ethylene glycol (EG) had a much higher effective thermal conductivity than either pure EG or EG containing the same volume fraction of dispersed metal-oxide nanoparticles. Choi et al. (2003) measured a 300% enhancement of thermal conductivity with 3 wt% loading of single-wall carbon nanotubes. The temperature dependence of k_{eff} for the polymer composites was also demonstrated in their experiments. In order to avoid aggregates, these carbon nanotubes have to be surface-treated, or, say, nitric acid has to be added to the mixture. In general, nanofluids overcome the drawbacks of liquids with large particles, i.e., rapid particle sedimentation, clogged flow channels, eroded conduits, and elevated pressure drops.

Although the experimental results have demonstrated a significant potential for thermal conductivity enhancement, the determination of the underlying physics is still in a primary stage, complicated by the fact that the available experimental data from different research group may vary significantly (see Koo and Kleinstreuer, 2003; among others). Clearly, nanoparticle volume fraction, physical characteristics and fluid type are important factors, but insufficient to explain the anomalous increase in thermal performance of nanofluids. Other reasons proposed include a very high particle-liquid interface conductivity due to molecular-size layering of the carrier fluid around the particles as well as Brownian motion of the nanoparticles causing micro-mixing. Additional mechanisms include the effect of nanoparticle clustering, the nature of heat transfer inside the particles, the interaction and collision among particles, thermal waves via hyperbolic heat conduction, and nanoparticle dispersion. Other nanoparticle-motion mechanisms, such as thermophoresis and osmophoresis, are negligible (Koo and Kleinstreuer, 2005a,b). Based on a molecular dynamics simulation, Sarkar and Selvam (2007) concluded that the thermal transport enhancement of nanofluids was mostly due to the increased movement of liquid atoms in the presence of nanoparticles. However, some researchers questioned the role of Brownian motion hydrodynamics for the unusual thermal effect of nanofluid (see Evans et al., 2006; Vladkov and Barrat, 2006; among others) as well as the actual k_{eff}-increase as reported in experimental papers (see Venerus et al., 2006; Putnam et al., 2006; Beck et al., 2007; among others).

Nevertheless, the hypothesis that Brownian motion of the nanoparticles causes micro-mixing has recently become more and more popular (see Koo and Kleinstreuer, 2004, 2005a,b; Jang and Choi, 2004, 2006, 2007; Prasher et al., 2006; among others). In a comparison study where Kleinstreuer and Li (in press) discussed the effective thermal conductivity theory of Jang and Choi (2004, 2006, 2007), it was found that their model cannot consistently match measured thermal performances of nanofluids, especially when the fluid temperature changes. Thus, to predict the thermal performance of nanofluids in microscale cooling devices and other thermal micro-systems, the influence of temperature on the effective thermal conductivity has to be considered.

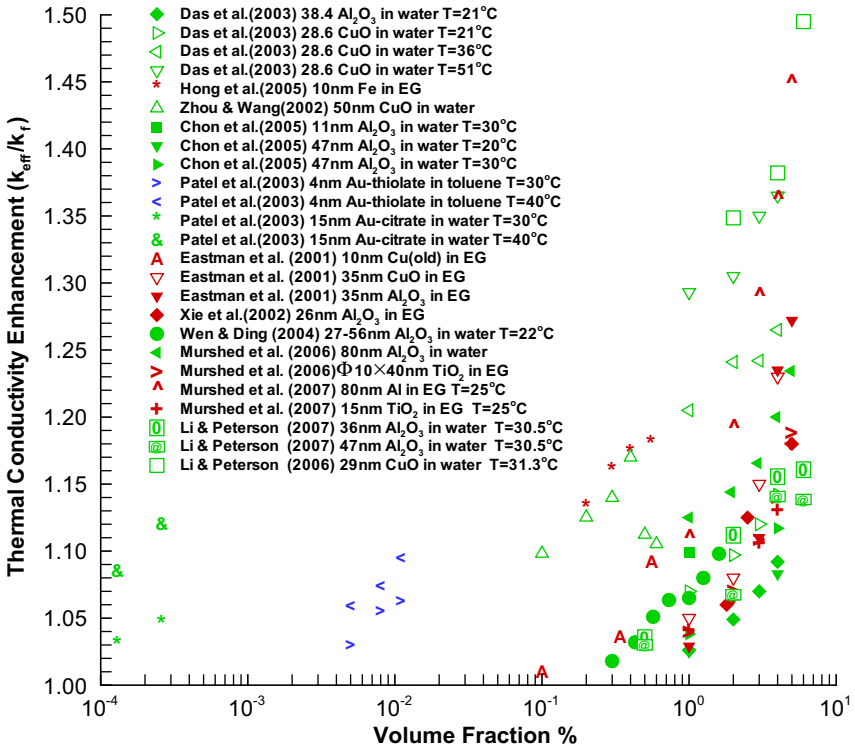

Fig. 1. Sample of experimental evidence for elevated k_{eff}/k_f of nanofluids.

2. Theory and analysis

Of interest is the use of a most suitable k_{eff} model for the computational analysis of nanofluid flow in a representative microchannel of a typical cooling device. Hence, first two competitive k_{eff} models are compared in light of benchmark experimental data sets. Then, pure water and nanofluid flow with heat transfer is investigated.

2.1. Temperature-dependent k_{eff} models for nanofluids

One possible k_{eff} correlation proposed by Prasher et al. (2006) is the multi-sphere Brownian model (MSBM) which can be described as follows. After having analyzed several possible thermal conduction mechanisms and associated models, Prasher et al. (2006) confirmed that the localized convection in the liquid due to Brownian movement of the particles is primarily responsible for the observed enhancement of the effective thermal conductivity of nanofluids. They captured random dispersions with a "Brownian-motion Reynolds number" based on the root-mean-square velocity of a Brownian particle as part of a modified Maxwell-Garnett thermal conductivity model (Nan et al., 1997), which also considers the influence of interfacial thermal resistance, R_b, between nanoparticles and different fluids. The description of multi-sphere convective interaction was borrowed from fluidized bed heat transfer (Brodkey et al., 1991). Combining these phenomena, the MSBM was proposed in the form:

$$\frac{k_{\text{eff}}}{k_{\text{f}}} = (1 + CRe^{m}Pr^{0.333}\varphi) \times \left(\frac{[k_{\text{p}}(1+2\alpha)+2k_{\text{m}}]+2\varphi[k_{\text{p}}(1-2\alpha)-k_{\text{m}}]}{[k_{\text{p}}(1+2\alpha)+2k_{\text{m}}]-\varphi[k_{\text{p}}(1-\alpha)-k_{\text{m}}]}\right) \quad (1)$$

where $Re = V_N d_p/v$, V_N is the root-mean-square velocity, v is the kinematic viscosity of the liquid, $\alpha = 2R_b k_m/d_p$ is the nanoparticle Biot number, R_b is the selective interfacial thermal resistance, k_m is the medium thermal conductivity, and C and m are adjustable constants; while C is independent of the fluid type, m depends on the fluid. For example, comparing the MSBM with data from water-based nanofluids and assuming R_b to be 0.77×10^{-8} km^2 W^{-1}, they calculated $C = 40{,}000$ and $m = 2.5 \pm 0.15$. Ethylene glycol (EG) and engine oil were also matched well when employing appropriate R_b and m values. As shown in Fig. 2, the MSBM model generates a good agreement with some of the recent Al_2O_3–water experimental data sets when employing a decent m value. However, the MSBM model can not predict the thermal conductivity enhancement trend for the experimental results of Li and Peterson (2007). Interestingly enough, the experimental data of Chon et al. (2005) also indicated a different trend while employing the same nanofluids, i.e., the same particle diameter and volume fraction. The MSBM comparisons were also not convincing when the particle was too small ($\leqslant$11 nm) or too large ($\geqslant$125 nm).

According to the postulate that submicron particle Brownian motion has explicitly a significant impact on the effective thermal conductivity, Koo and Kleinstreuer

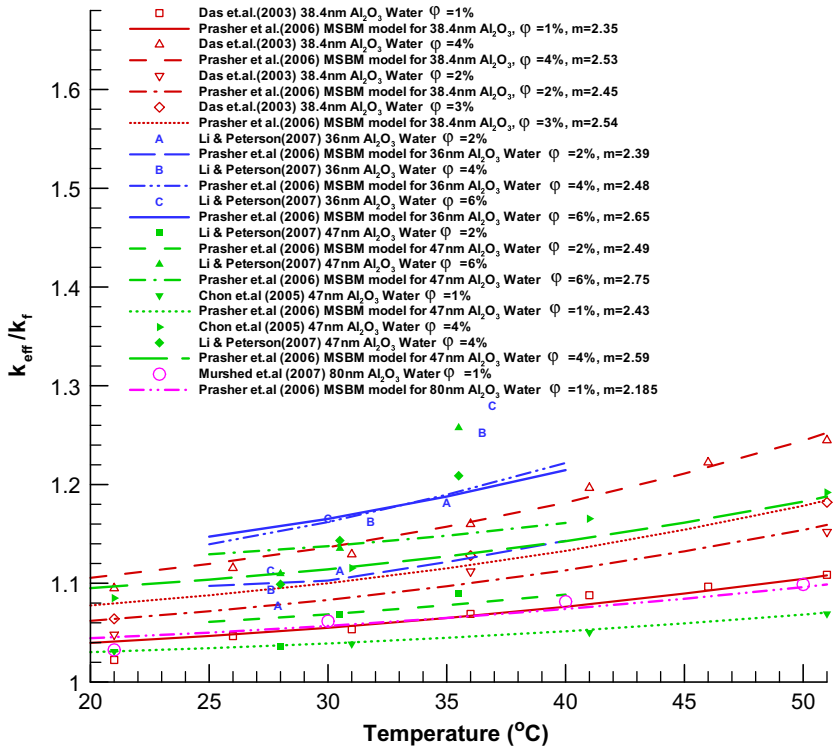

Fig. 2. Comparison of Prasher et al. (2006) thermal conductivity enhancement model (MSBM) with experimental data for Al_2O_3–water nanofluids at different temperatures.

(2004) proposed that k_{eff} is composed of the nanoparticle's conventional static part and a Brownian motion part. Their thermal conductivity model takes into account the effects of particle size, particle volume fraction and temperature dependence as well as type of nanoparticle and base fluid combinations. Specially,

$$k_{eff} = k_{static} + k_{Brownian} \tag{2}$$

where the static part is Maxwell's model and the dynamic part was developed based on kinetic theory together with Stokes' flow of micro-scale convective heat transfer, i.e., *micro-mixing*. Hence,

$$\frac{k_{static}}{k_f} = 1 + \frac{3\left(\frac{k_p}{k_f} - 1\right)\varphi}{\left(\frac{k_p}{k_f} + 2\right) - \left(\frac{k_p}{k_f} - 1\right)\varphi} \tag{3}$$

and

$$k_{Brownian} = 5 \times 10^4 \beta \varphi \rho_f c_{p,f} \sqrt{\frac{\kappa_b T}{\rho_p d_p}} f(T, \varphi) \tag{4}$$

The functions β and f, to be determined semi-empirically, were introduced to encapsulate the thermo-hydrodynamic interactions among micro-scale fluid parcels and the nanoparticle interactions capturing any temperature dependence (Koo and Kleinstreuer, 2005a,b). What is missing in Eq. (4) is the interfacial thermal resistance R_b between nanoparticles and base fluids (see Prasher et al., 2006; Jang and Choi, 2007; Xuan et al., 2006; Xue, 2006). The thermal interfacial resistance (also called Kapitza resistance) is believed to exist in the adjacent layers of the two different materials, i.e., the thin barrier layer plays a key role in weakening the effective thermal conductivity of the nanoparticles. For example, Wilson et al. (2002) reported that the magnitude of R_b between different nanoparticles and base fluids ranges from about $0.77 \times 10^{-8}\,km^2\,W^{-1}$ to approximately $20 \times 10^{-8}\,km^2\,W^{-1}$. More recently, Huxtable et al. (2003) showed that the interface thermal resistance across a carbon nanotube and base fluid is $8.33 \times 10^{-8}\,km^2\,W^{-1}$. Choosing an average value of $R_b = 4 \times 10^{-8}\,km^2\,W^{-1}$, the original K & K model was enhanced. In the static part, an effective nanoparticle thermal conductivity was used to substitute the isolated nanoparticle thermal conductivity, i.e.,

$$R_b + \frac{d_p}{k_p} = \frac{d_p}{k_{p,eff}} \tag{5}$$

The functions β and f in Eq. (4) were combined to a new g-function which considers the influence of multi-particle interaction which depends on particle diameter, temperature and volume fraction. For different base fluids and different nanoparticles, the g-function should differ; presently, only water-based nanofluids were considered because of the limits in available experimental data sets. For example, for Al_2O_3–water and CuO–water nanofluids, the nonlinear g-function generated r^2 values of 96% and 98%, respectively, using benchmark experimental data sets (Li, 2008)

Fig. 3 depicts a comparison of the new Koo–Kleinstreuer–Li (KKL) model with experimental data for Al_2O_3–water nanofluids at different temperatures. Similar

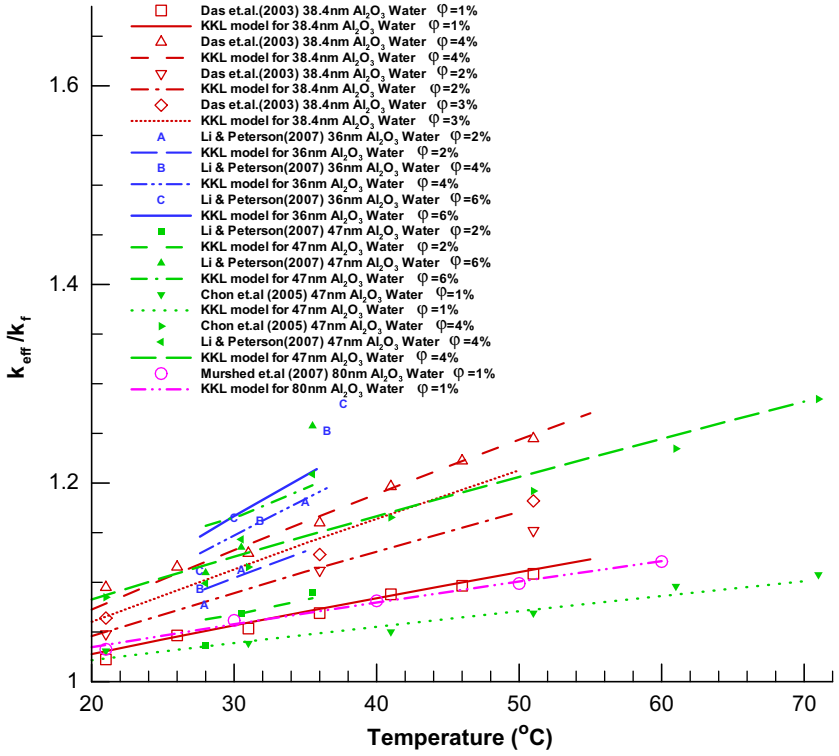

Fig. 3. Comparison of KKL model with experimental data for Al_2O_3–water nanofluids at different temperatures.

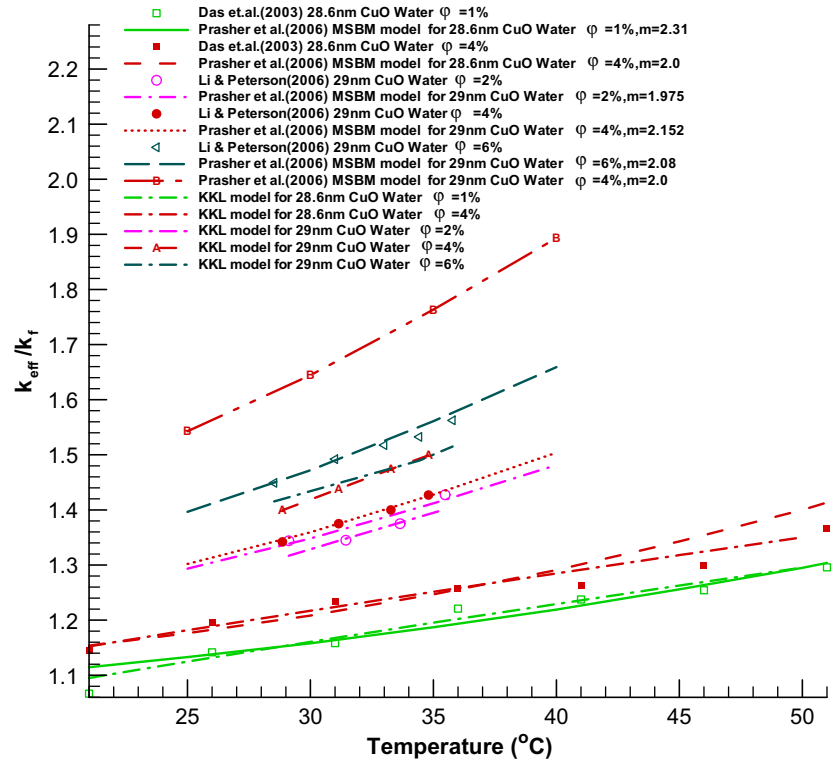

Fig. 4. Comparison of KKL model, MSMB model with experimental data for CuO–water nanofluids at different temperatures.

to the MSBM model, the KKL model shows a very good agreement with most of the recent experimental data sets. In Fig. 4, the KKL and MSBM models are compared with experimental data for CuO–water nanofluids at different temperatures. For the experimental data of Das et al. (2003), the KKL model provides a better matching than

the MSBM model, while the opposite is the case for the experimental data of Li and Peterson (2006). It must be mentioned that the m-value has an important influence on the MSBM model. If the value for the Reynolds number exponent is taken to be 2 for the 29 nm 4% CuO–water nanofluids, i.e., the same as for the 28.6 nm 4% CuO–water nanofluids, the predicted k_{eff} numbers generated by the MSBM model are far larger than the experiment values.

Both the Koo–Kleinstreuer–Li model and the MSBM model showed good agreements with most experimental results. The KKL model encapsulates micro-mixing due to random nanoparticle motion based on first principles. In contrast, the models by Jang and Choi (2007) and Prasher et al. (2006) contain Brownian motion effects implicitly in terms of "Brownian Reynolds numbers". Still, in the KKL theory, the complexities caused by multi-sphere interactions and strong temperature changes are lumped into a functional which could be detailed and expanded as more experimental evidence appears. The MSMB model employs adjustable parameters as well as factors C and m for data matching.

2.2. Pure water flow and nanofluid flow with heat transfer in a trapezoidal microchannel

Considering the strong temperature-dependent characteristics of the nanofluid thermal performance (see Figs. 2–4) and possibly large temperature differences in microheat sinks, temperature dependent physical properties of water and the new KKL model for the thermal conductivity of nanofluids were selected. Employing the commercial Navier–Stokes solver CFX-10 (Ansys Inc., Canonsburg, PA) and user-supplied pre- and post-processing software, pure water as well as CuO–water mixtures of different CuO-volume fractions were used as the working fluid.

Specifically, Fig. 5a depicts a representative microchannel as well as the associated computational mesh. The top width W_t, bottom width W_b and depth of the channel H are 500 μm, 358.4 μm and 100 μm, respectively (Chein and Chuang, 2005). The base angle, which is the angle between the channel side wall and bottom wall, is 54.7°. The length of the channel L is 27 mm. The heights of the cover and base substrate are both $H_c = 500$ μm. A constant heat flux of $q'' = 431{,}466\ \text{W/m}^2$ (10 W for the unit element) from below and adiabatic conditions at the other boundaries were assumed (Li et al., 2004). For comparison, first a smooth channel with pure de-ionized water as the working fluid was considered. The hydraulic diameter for the present case is:

$$D_h = \frac{4 \times 0.5 \times (W_t + W_b) \times H}{W_t + W_b + 2 \times H/\sin\theta} = 155.6\ \mu\text{m} \tag{6}$$

Other important geometric channel parameters are the aspect ratio as well as the aspect factor, defined respectively as

$$A_{ar} = W_b/W_t \text{ and } A_{af} = H/W_b \tag{7a, b}$$

The fluid material properties (density, thermal conductivity, dynamic viscosity, specific thermal capacity at constant pressure) were temperature dependent. For steady-state operations, the continuum mechanics equations are:

$$\nabla \cdot [\rho_f(T)\vec{u}] = 0 \tag{8}$$

$$\rho_f(\vec{u} \cdot \nabla\vec{u}) = -\nabla p + \nabla \cdot (\mu_f \nabla\vec{u}) \tag{9}$$

and

$$\rho_f c_{p,f}(\vec{u} \cdot \nabla T) = k_f \nabla^2 T + \mu_f \Phi \tag{10}$$

where

$$\Phi = \left(\frac{\partial u_i}{\partial x_j} + \frac{\partial u_j}{\partial x_i}\right)\frac{\partial u_i}{\partial x_j} \tag{11}$$

Here $\vec{u}$ is the velocity vector; and Φ is the viscous dissipation function. As hydraulic boundary conditions, a uniform velocity is applied at the channel inlet, i.e., $u_x = 0$, $u_y = 0$, $u_z = U_{in}$, u_x, u_y, and u_z are the velocity vector quantities in x, y, and z direction. The outlet pressure is the static pressure, i.e., $p_{out} = 0$. The no-slip boundary condition was enforced at all solid walls. The thermal boundary con-

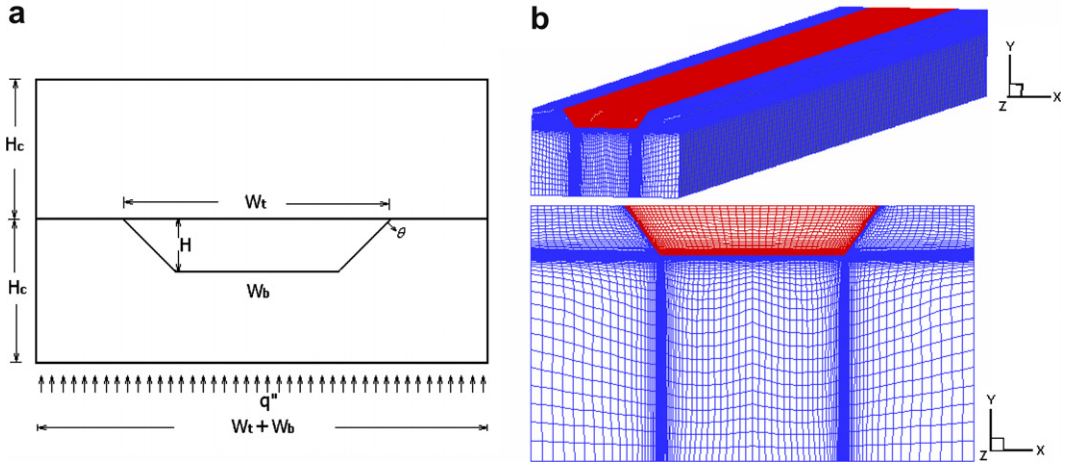

Fig. 5. (a) Typical microchannel heat sink (MCHS) element and (b) finite volume mesh.

dition at the bottom is $q'' = C$; adiabatic boundary conditions are applied at all other sides of the walls, $\frac{\partial T}{\partial n} = 0$; and $T = T_{in}$ in the fluid inlet region.

2.2.1. Pure water flow

For comparison purposes, a steady global energy balance based on the temperature difference between the channel inlet and outlet was performed, i.e.,

$$\rho_f u_m c_p A_c (T_{out} - T_{in}) = q'' \cdot A_{bottom} \tag{12}$$

Fig. 6 depicts the simulated water temperature rise between the channel inlet and outlet as a function of inlet Reynolds number and the theoretical values predicted by Eq. (12). In both of the two situations (scenarios, i.e., constant and temperature-dependent water properties), the simulation results match the energy balance predictions. The temperature difference between inlet and outlet are slightly higher when the water properties are dependent on the temperature especially for small Reynolds numbers. The reason is that water has a smaller thermal capacity at elevated fluid temperatures.

For noncircular conduits the channel aspect ratio or aspect factor (see Eq. (7a,b)) has a profound influence on the friction coefficient (or Poiseuille number):

$$C_f = f\,Re = \frac{\Delta p \cdot D_h^2}{2\mu_f u L} \tag{13}$$

which has a constant value of 16 for circular conduits. As shown in Fig. 7, the computed friction factor shows a good agreement with the empirical correlation of Wu and Cheng (2003) for fully develop flow, i.e.,

$$f\,Re = 11.43 + 0.80\exp(2.67 W_b/W_t) \tag{14}$$

For channel flow, the friction factor should be constant in the laminar flow regime. Indeed, the simulation result is almost parallel to the experimental empirical value within an error less than 3%. The simulation results for the temperature-dependent case are also within a 3% error margin. When the Reynolds number is larger than 1000, the theoretical friction factor hardly changes, i.e., the temperature differences in the fluid are small because of the relatively high mean velocities.

2.2.2. Nanofluid flow with heat transfer

In order to investigate the heat transfer characteristics of nanofluid flow in the trapezoidal microchannel, a CuO–water combination was used as the working fluid. Clearly, the thermal fluid properties of the nanofluid have to be updated. Thus, in the governing Eqs. (9) and (10), the following expressions were introduced, replacing the previous μ_f and k_f parameters. Typically, for a very dilute suspension, the effective viscosity, density and specific heat capacity have the following forms (Xuan and Roetzel, 2000):

$$\mu_{eff} = \mu_f \frac{1}{(1-\varphi)^{2.5}} \tag{15}$$

$$\rho_{eff} = \varphi\rho_p + (1-\varphi)\rho_f \tag{16}$$

$$(\rho c_p)_{eff} = \varphi(\rho c_p)_p + (1-\varphi)(\rho c_p)_f \tag{17}$$

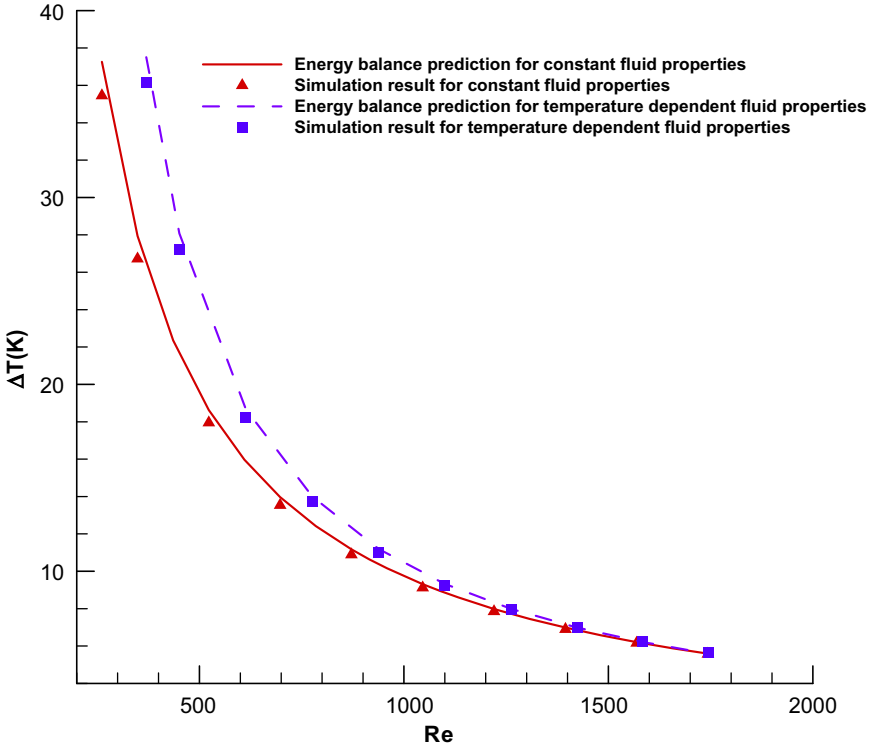

Fig. 6. Model validations: temperature rise from heat sink inlet to outlet.

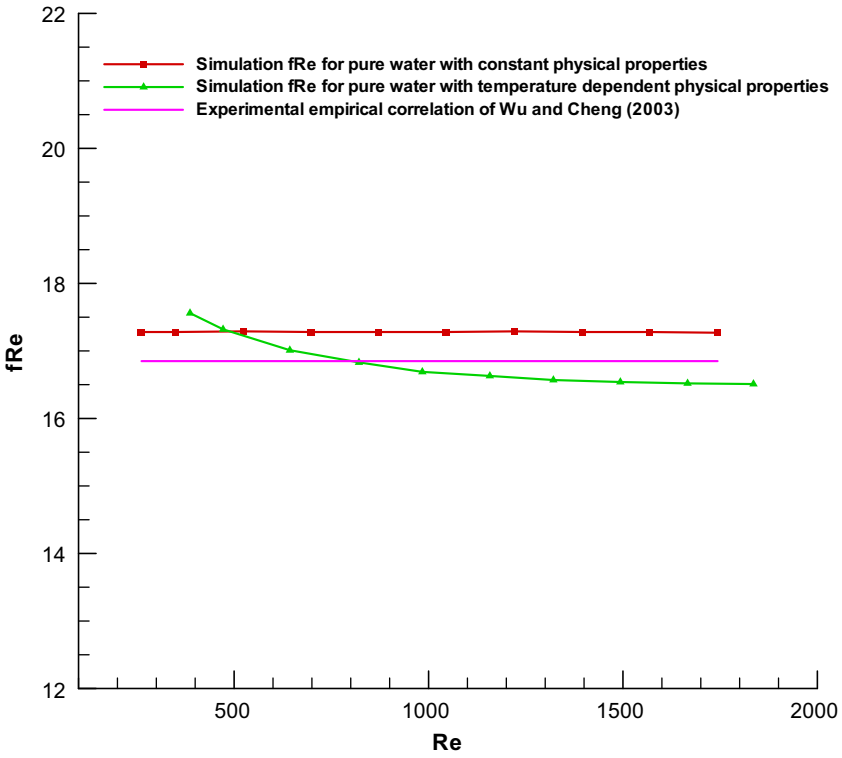

Fig. 7. Model validations: friction factors vs. Reynolds number.

here ρ_{eff} is the nanofluid density, μ_{eff} is the nanofluid viscosity, $(\rho c_p)_{\text{eff}}$ is the nanofluid specific heat capacity. For the effective thermal conductivity, the new KKL model (see Section 2.1) is employed.

The calculated fully-developed pressure gradient results for pure water and the CuO–water mixture at different volume fractions as a function of Reynolds number are given in Fig. 8. For the three cases, the Reynolds numbers differ even for same fluid entrance velocity, because of the different densities and dynamic viscosities. As expected, the trend shows a minor pressure gradient increase for the same Reynolds numbers when employing nanofluids. Specifically, the pressure gradient enhancement is less than 2% and 5% for CuO–water nanofluid with a volume fraction of 1% and 4%, respectively. Fig. 9 shows the pressure gradient increase at different mean velocities. The enhancement is less than 5% for CuO–water with a volume fraction of 1%, while for CuO–water with a volume fraction of 4% the increase is up to 15%.

Pumping power is needed to drive the working fluid in microchannels, which is defined as the product of the pressure drop across the channel (Δp) and volumetric flow rate (Q), i.e.,

$$P = \Delta p \cdot Q \tag{18}$$

As is shown in Fig. 10, there is not much difference in pressure drops when using pure water and nanofluids. There is an average 2% increase for CuO–water with a 1% volume fraction and an average 8% enhancement for the CuO–water with a 4% volume fraction. Thus, it does not need require additional pumping power to drive nanofluid flow, especially for lower particle volume fractions. Chein and Chuang (2005) showed similar phenomena based on theoretical models and experimental correlations.

In order to investigate heat transfer enhancement for nanofluids, the average Nusselt numbers for different volume fractions were compared. The average Nusselt number is defined as

$$Nu_{\text{ave}} = \frac{q'' \cdot D_{\text{h}}}{(T_{\text{w,ave}} - T_{\text{f,ave}})k_{\text{f}}} \tag{19}$$

where $T_{\text{w,ave}}$ is the surface-averaged temperature at the fluid–solid interface of area A_{int}, $T_{\text{f,ave}}$ is the volume-averaged temperature of the fluid field. Fig. 11 compares the average Nusselt number for pure water flow and CuO–water nanofluid flow with different volume fractions. It demonstrates that nanofluids can improve the thermal performance of microchannels: (i) the larger the volume fraction of nanoparticles, the higher is the thermal performance; (ii) a volume fraction of 1% CuO–water nanofluid shows an average 15% enhancement of thermal performance, when the volume fraction increases to 4%, there is a 20% increase over that of pure water.

In order to compare the thermal performance of nanofluids, the thermal resistance is employed:

$$\theta = \frac{T_{\text{w,ave}} - T_{\text{in}}}{q} \tag{20}$$

where T_{in} is the fluid inlet temperature and q is the heat added to the microchannel. As shown in Fig. 12, the thermal

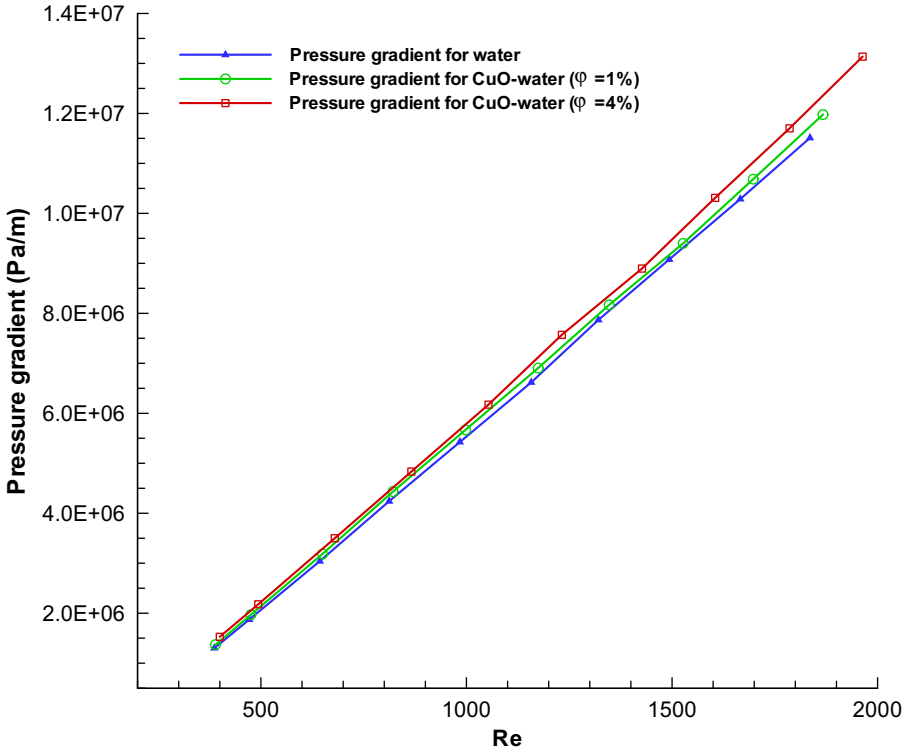

Fig. 8. Computational results: pressure gradient vs. Reynolds number.

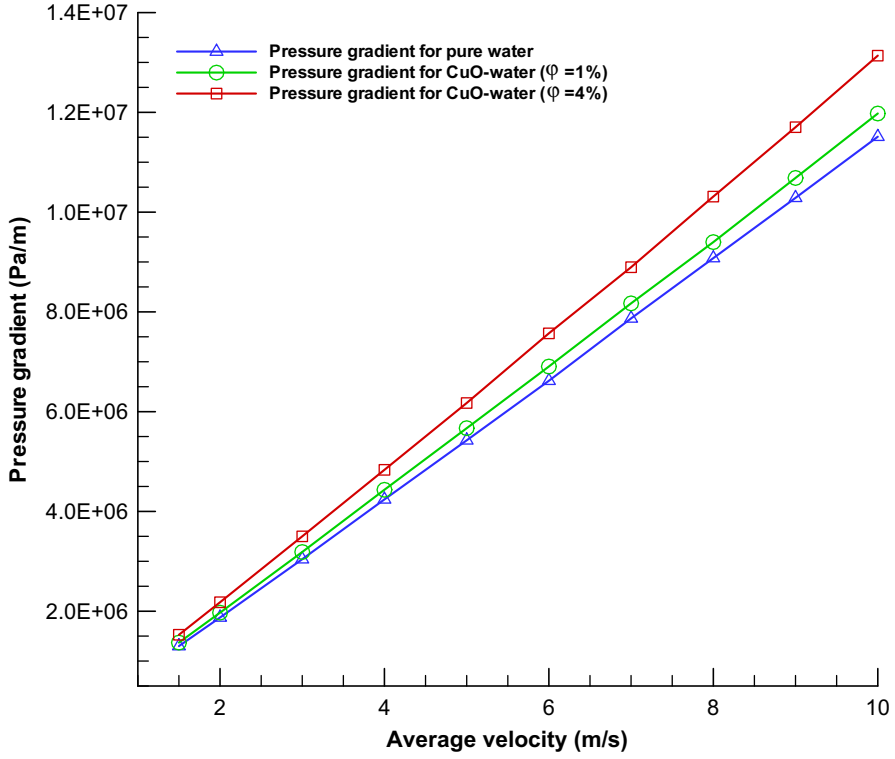

Fig. 9. Computational results: pressure gradient vs. mean velocity.

performance is enhanced when employing nanofluids. The average enhancement of thermal performance for CuO–water with a volume fraction of 1% is about 11% and the increase is about 15% when the volume fraction is 4%.

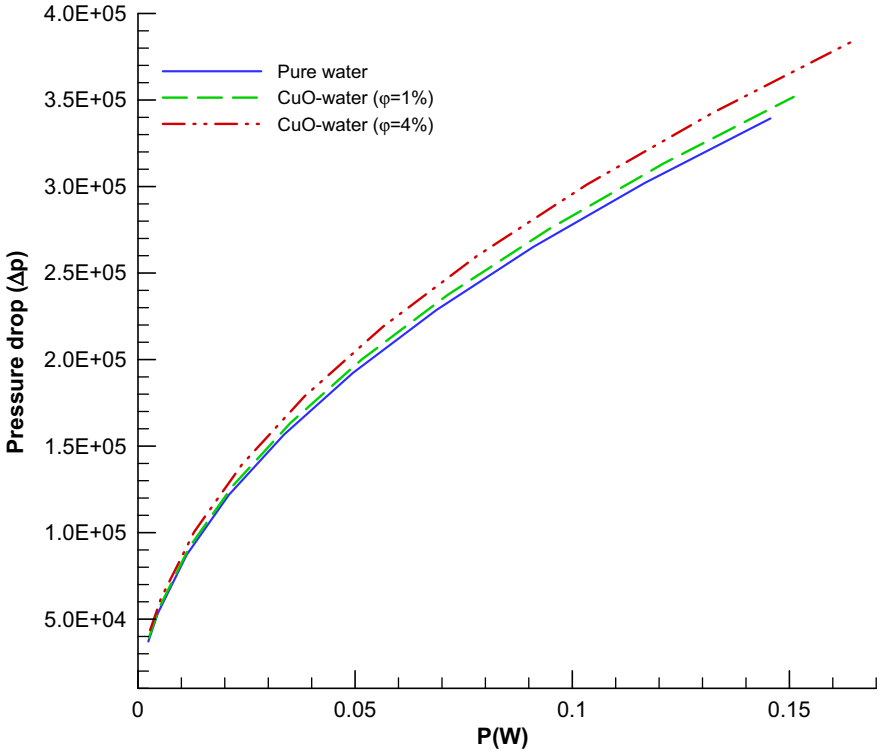

Fig. 10. Computational results: pressure drop vs. pumping power.

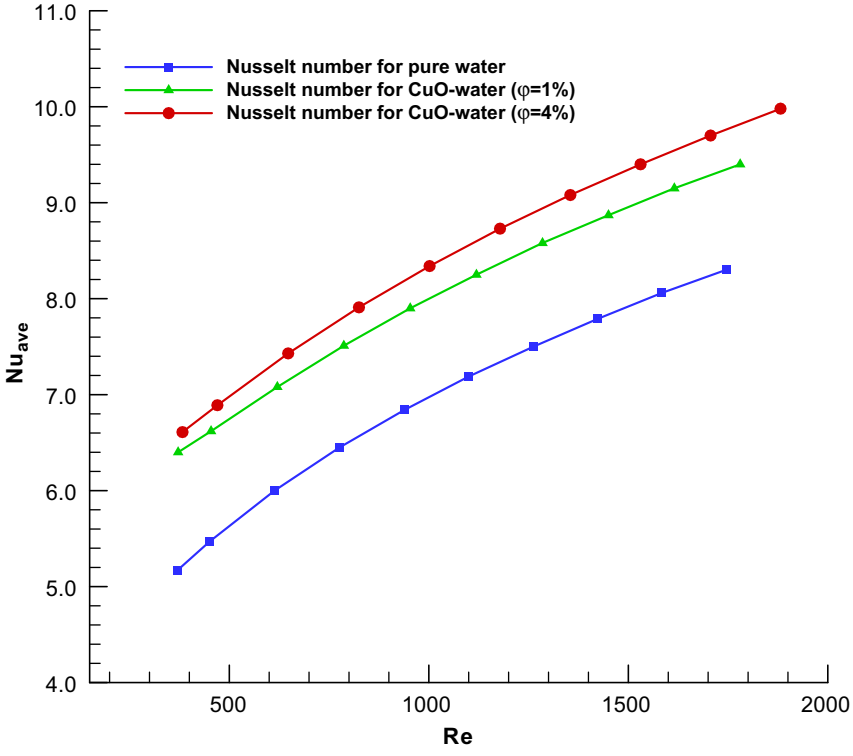

Fig. 11. Computational results: average Nusselt number vs. Reynolds number.

As depicted from Figs. 8, 10–12, nanofluids lower the thermal resistance and hence measurably enhance the performance of microchannels with little pumping power added. In summary, microchannel heat sinks with nano-

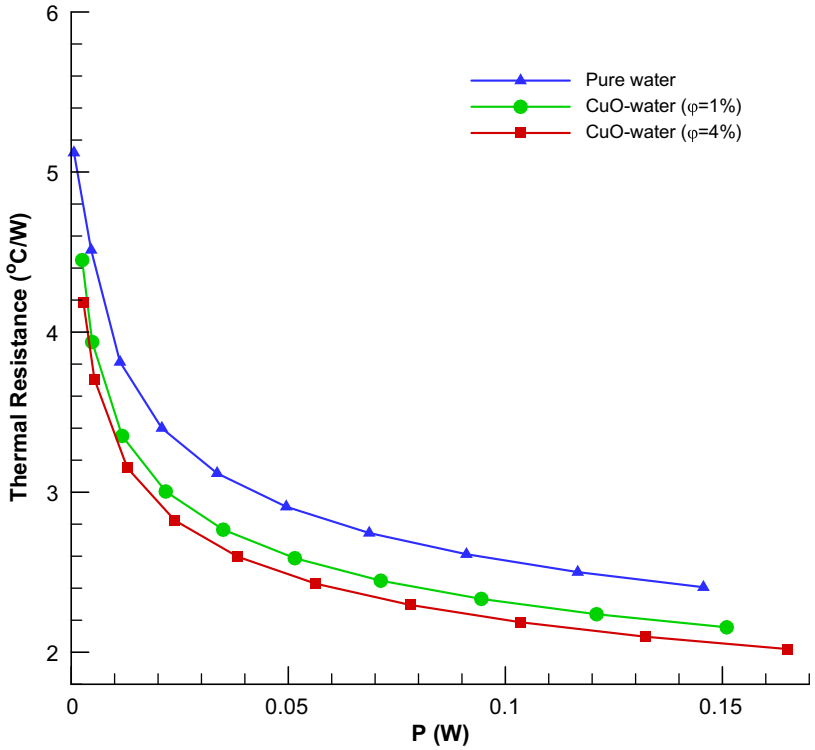

Fig. 12. Computational results: thermal resistance vs. pumping power.

fluids as coolant will be good candidates for the next generation of cooling devices.

3. Conclusions

Two effective thermal conductivity models for nanofluids were compared in detail, where the new KKL (Koo–Kleinstreuer–Li) model, based on Brownian-motion induced micro-mixing, achieved good agreements with the currently available experimental data sets. Employing the commercial Navier–Stokes solver CFX-10 (Ansys Inc., Canonsburg, PA) and user-supplied pre- and post-processing software, the thermal performance of nanofluid flow in a trapezoidal microchannel was analyzed using pure water and CuO–water with volume fractions of 1% and 4%. The results show that nanofluids do measurably enhance the thermal performance of microchannel mixture flow with a small increase in pumping power. The thermal performance increases with volume fraction; but, the extra pressure drop, or pumping power, will somewhat decrease the beneficial effects. Microchannel heat sinks with nanofluids are expected to be good candidates for the next generation of cooling devices.

References

Beck, M.P., Sun, T., Teja, A.S., 2007. The thermal conductivity of alumina nanoparticles dispersed in ethylene glycol. Fluid Phase Equilibria 260, 275–278.

Brodkey, R.S., Kim, D.S., Sidner, W., 1991. Fluid to particle heat transfer in a fluidized bed and to single particles. International Journal Heat and Mass of Transfer 34, 2327–2337.

Chang, H., Lo, C.H., Tsung, T.T., Cho, Y.Y., Tien, D.C., Chen, L.C., Thai, C.H., 2005. Temperature effect on the stability if CuO nanofluids based on measured particle distribution. Key Engineering Materials 295–296, 51–56.

Chein, R., Chuang, J., 2005. Analysis of microchannel heat sink performance using nanofluids. Applied Thermal Engineering 25, 3104–3114.

Choi, E.S., Brooks, J.S., Eaton, D.L., Al-Haik, M.S., Hussaini, M.Y., Garmestani, H., Li, D., Dahmen, K., 2003. Enhancement of thermal and electrical properties of carbon nanotube polymer composites by magnetic field processing. Journal of Applied Physics 94 (9), 6034–6039.

Choi, S.U.S., 1995. Enhancing thermal conductivity of fluids with nanoparticles. In: Sininer, D.A., Wang, H.P. (Eds.), Developments and Applications of Non-Newtonian Flows, ASME, New York, FED-vol. 231/MD-Vol. 66.

Chon, C.H., Kihm, K.D., Lee, S.P., Choi, S.U.S., 2005. Empirical correlation finding the role of temperature and particle size for nanofluid (Al_2O_3) thermal conductivity enhancement. Applied Physics Letters 87, 15107, pp. 153107-1–153107-3.

Chopkar, M., Kumar, S., Bhandari, D.R., Das, P.K., Manna, I., 2007. Development and characterization of $Al_{70}Cu_{30}$ and $Al_{70}Ag_{30}$ nanoparticle dispersed water and ethylene glycol based nanofluids. Materials Science and Engineering B 139, 141–148.

Das, S.K., Putra, N., Thiesen, P., Roetzel, W., 2003. Temperature dependence of thermal conductivity enhancement for nanofluids. Journal of Heat Transfer 125, 567–574.

Eastman, J.A., Choi, S.U.S., Li, S., Yu, W., Thompson, L.J., 2001. Anomalously increased effective thermal conductivities of ethylene glycol-based nanofluids containing copper nanoparticles. Applied Physics Letters 78 (6), 718–720.

Evans, W., Fish, J., Keblinski, P., 2006. Role of Brownian motion hydrodynamics on nanofluid thermal conductivity. Applied Physics Letter 88, 093116-1-3.

Hong, T.-K., Yang, H.-S., Choi, C.J., 2005. Study of the enhanced thermal conductivity of Fe nanofluids. Journal of Applied Physics 97, 064311.

Huxtable, S.T., Cahill, D.G., Shenogin, S., et al., 2003. Interfacial heat flow in carbon nanotube suspensions. Nature Materials 2, 731–734.

Jang, S.P., Choi, S.U.S., 2004. The role of Brownian motion in the enhanced thermal conductivity of nanofluids. Applied Physics Letters 84, 4316–4318.

Jang, S.P., Choi, S.U.S., 2006. Cooling performance of a microchannel heat sink with nanofluids. Applied Thermal Engineering 26, 2457–2463.

Jang, S.P., Choi, S.U.S., 2007. Effects of various parameters on nanofluid thermal conductivity. Journal of Heat transfer 129, 617–623.

Kleinstreuer, C., Koo, J., 2004. Computational analysis of wall roughness effects for liquid flow in micro-conduits. ASME Journal of Fluid Engineering 126, 1–9.

Kleinstreuer, C., Li, J., 2007. Microscale cooling devices, to appear In: Li, D. (Ed.), Encyclopedia of Micro and Nanofluidic, Springer-Verlag, Heidelberg, DE.

Kleinstreuer, C., Li, J., in press. Analysis of the Jang & Choi k_{eff}-model. ASME Journal of Heat Transfer.

Koo, J., 2004, Computational nanofluid flow and heat transfer analyses applied to micro-systems, Ph.D Thesis, NC State University, Raleigh, NC.

Koo, J., Kleinstreuer, C., 2003. Liquid flow in microchannels: experimental observations and computational analysis of microfluidics effect. Journal of Micromechanics and Microengineering 13, 568–579.

Koo, J., Kleinstreuer, C., 2004. A new thermal conductivity model for nanofluids. Journal of Nanoparticle Research 6, 577–588.

Koo, J., Kleinstreuer, C., 2005a. Laminar nanofluid flow in microheat-sinks. International Journal of Heat and Mass Transfer 48, 2652–2661.

Koo, J., Kleinstreuer, C., 2005b. Impact analysis of nanoparticle motion mechanisms on the thermal conductivity of nanofluids. International Communications in Heat and Mass Transfer 32, 1111–1118.

Lee, S., Choi, S.U.S., Li, S., Eastman, J.A., 1999. Measuring thermal conductivity of fluids containing oxide nanoparticles. Journal of Heat Transfer – Transactions of the ASME 121 (2), 280–289.

Li, C.H., Peterson, G.P., 2007. The effect of particle size on the effective thermal conductivity of Al_2O_3–water nanofluids. Journal of Applied Physics 101, 044312.

Li, C.H., Peterson, G.P., 2006. Experimental investigation of temperature and volume fraction variations on the effective thermal conductivity of nanoparticle suspensions (nanofluids). Journal of Applied Physics 99, 084314.

Li, J., 2008. Computational analysis of nanofluid flow in microchannels with applications to micro-heat sinks and bio-MEMS, Ph.D. dissertation, MAE department, NCSU, Raleigh, NC.

Li, J., Peterson, G.P., Cheng, P., 2004. Three-dimensional analysis of heat transfer in a micro-heat sink with single phase flow. International Journal of Heat and Mass Transfer 47, 4215–4231.

Masuda, H., Ebata, A., Teramae, K., Hishinuma, N., 1993. Alteration of thermal conductivity and viscosity of liquid by dispersing ultra-fine particles (dispersion ofγ-Al_2O_3,SiO_2 and TiO_2 ultra-fine particles). Netsu Bussei 4, 227–233.

Murshed, S.M.S., Leong, K.C., Yang, C., 2006. A model for predicting the effective thermal conductivity of nanoparticle-fluid suspensions. International Journal of Nanoscience 5, 23–33.

Murshed, S.M.S., Leong, K.C., Yang, C., in press. Investigations of thermal conductivity and viscosity of nanofluids. International Journal of Thermal Sciences.

Nan, C.-W., Birringer, R., Clarke, D.R., Gleiter, H., 1997. Effective thermal conductivity of particulate composites with interfacial thermal resistance. Journal of Applied Physics 81, 6692–6699.

Patel, H.E., Das, S.K., Sundararajan, T., Nair, A.S., George, B., Pradeep, T., 2003. Thermal conductivities of naked and monolayer protected metal nanoparticle based nanofluids: manifestation of anomalous enhancement and chemical effect. Applied Physics Letters 83, 2931–2933.

Prasher, R.S., Bhattacharya, P., Phelan, P.E., 2006. Brownian motion based convective conductive model for the effective thermal conductivity of nanofluids. Journal of Heat Transfer 128, 588–595.

Putnam, S.A., Cahill, D.G., Braun, P.V., Ge, Z., Shimmin, R.G., 2006. Thermal conductivity of nanoparticle suspensions. Journal of Applied Physics 99, 084308-1–084308-6.

Sarkar, S., Selvam, R.P., 2007. Molecular dynamics simulation of effective thermal conductivity and study of enhanced thermal transport mechanism in nanofluids. Journal of Applied Physics 102, 074302-1-7.

Venerus, D.C., Kabadi, M.S., Lee, S., Peres-Luna, V., 2006. Study of thermal transport in nanoparticle suspensions using forced Rayleigh scattering. Journal of Applied Physics 100, 094310-1-5.

Vladkov, M., Barrat, J.L., 2006. Modeling transient absorption and thermal conductivity in a simple nanofluid. Nanoletters 6 (6), 1224–1228.

Wen, D., Ding, Y., 2004. Experimental investigation into convective heat transfer of nanofluids at the entrance region under laminar flow conditions. International Journal of Heat and Mass Transfer 47, 5181–5188.

Wilson, O.M., Hu, X., Cahill, D.G., Braun, P.V., 2002. Colloidal metal particles as probes of nanoscale thermal transport in fluids. Physical Review B 66, 224301-1-6.

Wu, H.Y., Cheng, P., 2003. Friction factors in smooth trapezoidal silicon microchannels with different aspect ratios. International Journal of Heat and Mass Transfer 46 (14), 2519–2525.

Xie, H.Q., Wang, J.C., Xi, T.G., Liu, Y., Ai, F., Wu, Q., 2002. Thermal conductivity enhancement of suspensions containing nanosized alumina particles. Journal of Applied Physics 91 (7), 4568–4572.

Xuan, Y., Li, Q., Zhang, X., Fujii, M., 2006. Stochastic thermal transport of nanoparticle suspensions. Journal of Applied Physics 100, 043507.

Xuan, Y., Roetzel, W., 2000. Conceptions for heat transfer correlation of nanofluids. International Journal of Heat Mass Transfer 43, 3701–3707.

Xue, Q.Z., 2006. Model for the effective thermal conductivity of carbon nanotube composites. Nanotechnology 17, 1655–1660.

Zhou, L.P., Wang, B.X., 2002. Experimental research on the thermo-physical properties of nanoparticle suspensions using the quasi-steady method. Annual Proceeding of Chinese Engineering Thermophysics. pp. 889–892 (in Chinese).

Further reading

Hong, T.-K., Yang, H.-S., Choi, C.J., 2005. Study of the enhanced thermal conductivity of Fe nanofluids. Journal of Applied Physics 97, 064311.

Kleinstreuer, C., Koo, J., 2004. Computational analysis of wall roughness effects for liquid flow in micro-conduits. ASME Journal of Fluid Engineering 126, 1–9.

Kleinstreuer, C., Li, J., 2007. Microscale cooling devices, to appear In: Li, D. (Ed.), Encyclopedia of Micro and Nanofluidic, Springer-Verlag, Heidelberg, DE.

Koo, J., 2004, Computational nanofluid flow and heat transfer analyses applied to micro-systems, Ph.D Thesis, NC State University, Raleigh, NC.

Murshed, S.M.S., Leong, K.C., Yang, C., 2006. A model for predicting the effective thermal conductivity of nanoparticle-fluid suspensions. International Journal of Nanoscience 5, 23–33.

Murshed, S.M.S., Leong, K.C., Yang, C., in press. Investigations of thermal conductivity and viscosity of nanofluids. International Journal of Thermal Sciences.

Patel, H.E., Das, S.K., Sundararajan, T., Nair, A.S., George, B., Pradeep, T., 2003. Thermal conductivities of naked and monolayer protected metal nanoparticle based nanofluids: manifestation of anomalous enhancement and chemical effect. Applied Physics Letters 83, 2931–2933.

Wen, D., Ding, Y., 2004. Experimental investigation into convective heat transfer of nanofluids at the entrance region under laminar flow conditions. International Journal of Heat and Mass Transfer 47, 5181–5188.